This is a preprint of: "Period function for a family of piecewise planar Hamiltonian systems", Alex Carlucci Rezende, Mirianne A. S. Santos, Joan Torregrosa, *Internat. J. Bifur. Chaos Appl. Sci. Engrg.*, vol. 34(16), 2450199 (12 pp.), 2024.
DOI: [10.1142/S0218127424501992]

PERIOD FUNCTION FOR A FAMILY OF PIECEWISE PLANAR HAMILTONIAN SYSTEMS

ALEX C. REZENDE*
Departamento de Matemática, Universidade Federal de São Carlos (UFSCar), São Carlos, São Paulo, 13565-905, Brazil
alexcr@ufscar.br

MIRIANNE A. S. SANTOS
Departamento de Matemática, Universidade Federal de São Carlos (UFSCar), São Carlos, São Paulo, 13565-905, Brazil
mirianneandressa@gmail.com

JOAN TORREGROSA
Departament de Matemàtiques, Universitat Autònoma de Barcelona (UAB), Bellaterra, 08193, Barcelona, Spain;
Centre de Recerca Matemàtica, Campus de Bellaterra, Bellaterra, 08193, Barcelona, Spain
joan.torregrosa@uab.cat

In this paper, we analyze the monotonicity and the number of critical periods of the period function associated to a family of piecewise planar continuous potential systems. In particular, we describe the bifurcation diagram of the period function, determining the regions of the parameter space where it is monotonically increasing or decreasing and where it has at most one simple critical period. In order to prove the main result, we use that such a function can be written in terms of the two period functions of the uncoupled planar Hamiltonian systems matched by the separation line.

Keywords: Piecewise planar Hamiltonian systems, Period function, Monotonicity, Critical period, Bifurcation diagram.

1. Introduction and statement of the main results

There exist several papers dealing with properties of the period function, here denoted by T, in smooth Hamiltonian vector fields with respect to the monotonicity and the number of critical periods, i.e. the number of zeros of the derivative of T. In [Mañosas & Villadelprat, 2006] the authors analyzed the period function of the center singularity at the origin of the planar potential differential system associated to the Hamiltonian function $H(x, y) = y^2/2 + V(x)$, where $V(x) = x^2/2 + ax^4/4 + bx^6/6$, with $a, b \in \mathbb{R}$ and $b \neq 0$, as a continuation of the study carried out in [Chow & Sanders, 1986; Gavrilov, 1993], where $V(x) =$

*Corresponding author.

$x^2/2 + ax^3/3 + bx^4/4$. Such studies were made thanks to the qualitative properties of the corresponding Picard–Fuchs equations.

There also exist several contributions for piecewise differential systems in the sense of the conditions for the origin to be either a center or an isochronous center as in [Chen & Zhang, 2012; Coll *et al.*, 1999; Gasull & Torregrosa, 2003; Li *et al.*, 2015; Mañosas & Torres, 2005]. Moreover, there exist studies aiming to determine the number of critical periods of piecewise linear systems as in [Wang & Yang, 2020]. In [Mañosas & Torres, 2005] it is proved that for any analytical function F at the origin, with $F(0) = F'(0) = 0$ and $|F''(0)| < 1$, the piecewise system

$$(\dot{x}, \dot{y}) = \begin{cases} \big(-y, x + F'(x)\big), & \text{if } y \geq 0, \\ \big(-y, x - F'(x)\big), & \text{if } y < 0, \end{cases}$$

is a center if and only if $F(x)$ is even. Moreover, there is no non-trivial even function $F(x)$ such that the potentials $V^{\pm}(x) = x^2/2 \pm F(x)$ are isochronous and it is not possible to generate a non-trivial isochronous center by matching two centers generated by potentials $V^{\pm}(x)$, with $F(x) = \sum_{n\geq 3} a_n x^n$ an analytic non-linear function. The authors of [Mañosas & Torres, 2005] also consider piecewise planar differential systems

$$(\dot{x}, \dot{y}) = \begin{cases} \big(-y, F'(x)\big), & \text{if } y \geq 0, \\ \big(-y, G'(x)\big), & \text{if } y < 0, \end{cases} \tag{1}$$

where $F(x) = ax^2 + O(x^4)$, with $a > 0$ an analytic even function at 0. They proved that, for every $b > 0$, there exists a unique even function $G(x)$, analytic at the origin, such that $G(x) = bx^2 + O(x^4)$, for which the corresponding system (1) has an isochronous center at the origin.

However, in this paper we characterize the behavior of the period function, with respect to the monotonicity and the number of critical periods of the center at the origin for a family of piecewise planar Hamiltonian systems whose phase plane is composed by two uncoupled smooth systems matched by the line $x = 0$. More precisely, we obtain the bifurcation diagram of the period function associated to the family of piecewise continuous planar Hamiltonian differential systems given by

$$(\dot{x}, \dot{y}) = \begin{cases} (y, -x - ax^3), & \text{if } x \leq 0, \\ (y, -x - bx^3), & \text{if } x \geq 0, \end{cases} \tag{2}$$

where a and b are real numbers, whose Hamiltonian function is

$$H(x, y) = \frac{1}{2}y^2 + V(x), \tag{3}$$

where

$$V(x) = \begin{cases} V^-(x) = x^2/2 + ax^4/4, & \text{if } x \leq 0, \\ V^+(x) = x^2/2 + bx^4/4, & \text{if } x \geq 0. \end{cases} \tag{4}$$

That is, the solutions of system (2) are contained in the level curves of (3). We remark that it is not necessary to consider the classical definition of Filippov vector field (see [Filippov, 1988]), because the vector field associated to (2) is continuous.

In the case that the origin of family (2) is a center, the *period annulus* is the largest neighborhood $\mathcal{P}$ of such a point where each trajectory is a periodic function and its boundary is denoted by $\partial\mathcal{P}$. We denote by h_0 the level curve of the Hamiltonian function (3) that contains $\partial\mathcal{P}$. Moreover, if $h_0 < \infty$, then $\mathcal{P}$ is bounded, otherwise $\mathcal{P}$ is the whole plane and the center is global.

Similar to what is done for the continuous case, in piecewise Hamiltonian systems the periodic orbits in the period annulus can be parametrized by the energy (see [Cima *et al.*, 1999], for instance). For each $h \in [0, h_0)$, we denote by γ_h the set of points in $\mathbb{R}^2$ that verifies $H(x, y) = h$, where H is defined by (3). The function that associates each γ_h to its minimum period is said to be the *period function* and it is denoted by $T(h)$. Therefore, $T(h)$ is defined in $[0, h_0)$. We say that a center is *isochronous*, if the period function is constant.

The next result, which will be proved in Sec. 3, states that there exist four topologically different phase portraits for system (2), but only three different period annuli, and they are called, respectively, global center, saddle loop, and two saddle cycle; they are drawn in Fig. 1.

Proposition 1. *System* (2) *has a center at the origin and the following statements hold:*

(i) *For $a \geq 0$ and $b \geq 0$, it has only one equilibrium point at the origin, which is a global center (i.e. $h_0 = \infty$);*
(ii) *For $a \geq 0$ and $b < 0$ or $a < 0$ and $b \geq 0$, it has two equilibrium points, which are a center and a saddle point, and $\partial\mathcal{P}$ is a finite homoclinic connection in $h_0 = \max\{-1/(4a), -1/(4b)\}$;*
(iii) *For $a < 0$, $b < 0$, and $|a| \neq |b|$, it has three equilibrium points, which are a center and two saddles, and $\partial\mathcal{P}$ is a finite homoclinic connection in $h_0 = \min\{-1/(4a), -1/(4b)\}$;*
(iv) *For $a < 0$, $b < 0$ and $|a| = |b|$, it has three equilibrium points, which are a center and two saddle points, and $\partial\mathcal{P}$ is a finite heteroclinic connection in $h_0 = -1/(4a) = -1/(4b)$.*

The phase portraits for each item (i) to (iv) are topologically equivalent, respectively, to those ones presented in Fig. 1.

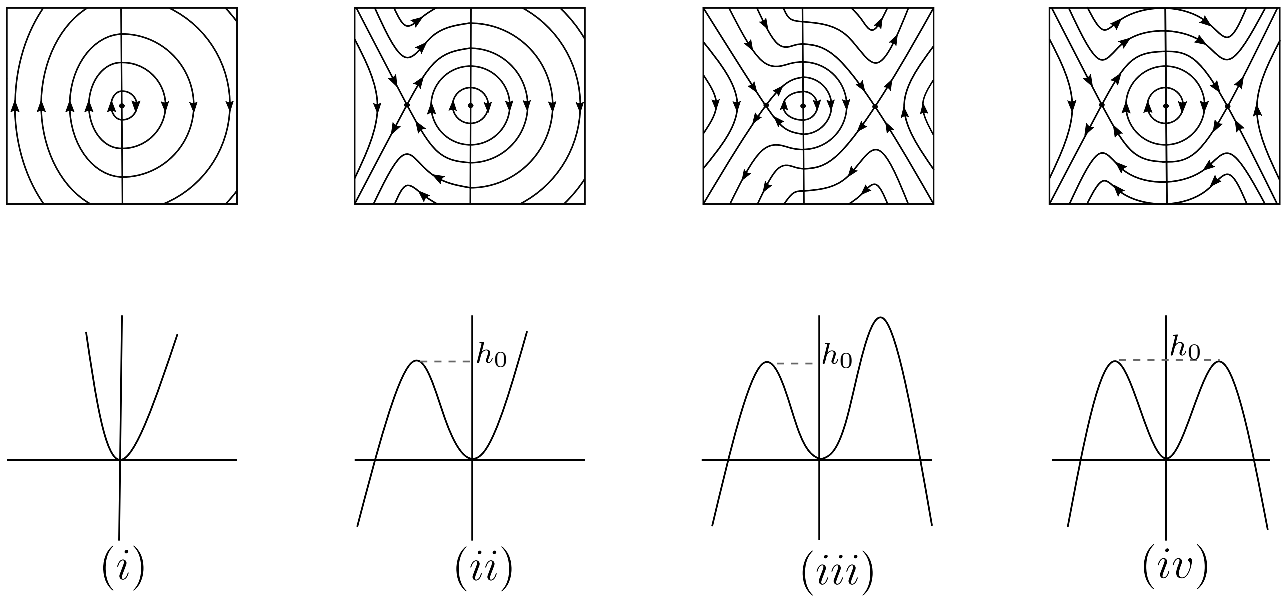

Fig. 1. Phase portraits for family (2) and graphic of V in (4)

It is clear from Proposition 1, that for each case we can define only one period function, since in all of them there exists only one region which is entirely covered by periodic orbits. Moreover, the domain of the period function is also detailed. The following result, proved in the last section, gives us information about the monotonicity and critical periods, when they exist, of such a function.

Theorem 1. *The period function of system* (2) *defined in* $[0, h_0)$ *satisfies the following conditions:*

(i) *For $a = b = 0$, it is constant;*
(ii) *For $a \geq 0$ and $b \geq 0$, not simultaneously zero, it is monotonically decreasing;*
(iii) *For $a < 0$ and $b < 0$, or $ab < 0$ with $|\min\{a, b\}| \geq \max\{a, b\}$, it is monotonically increasing;*
(iv) *For $ab < 0$ with $|\min\{a, b\}| < \max\{a, b\}$, it has one simple critical period at a minimum point.*

In what follows, we use the symbol $f'(h)$ to denote the derivative of a given function f with respect to the variable h. As discussed previously, if there exists an $h^* \in [0, h_0)$ such that $T'(h^*) = 0$, then $T(h^*)$ is called a *critical period*. If h^* is a simple zero of $T'(h)$, then $T(h^*)$ is called a *simple critical period*. From Theorem 1 we see that the period function can have at most one simple critical period for family (2).

Remark 1.1. System (2) is symmetric with respect to both x-axis and y-axis. In fact, using the transformation $(x, y, t) \mapsto (-x, -y, t)$, we obtain this double symmetry, which helps in calculating the period function.

As we will show in Sec. 4, the key point is that the period function $T(h)$ of system (2) can be expressed as the sum of the halves of the periods of the two uncoupled planar Hamiltonian systems matched by the separation line $x = 0$, because of the symmetry described in the above remark. So, it is natural to study each zone separately unifying the notation as follows:

$$(\dot{x}, \dot{y}) = (y, -x - cx^3), \tag{5}$$

with c a real parameter, associated to the Hamiltonian function

$$H(x, y) = \frac{y^2}{2} + \frac{x^2}{2} + \frac{cx^4}{4}, \tag{6}$$

Even though the monotonicity of the period function of (5) has already been studied in [Chicone, 1987; Chow & Sanders, 1986; Gasull *et al.*, 1997], as usual in nonsmooth context, we cannot take the benefit of such individual studies to obtain directly all the properties proved in this paper. Because the number of oscillations of the sum of two monotonically increasing and decreasing functions is unpredictable a priori. Hence, for completeness, we present in Sec. 2 the study of the behavior of the period function for system (5) following closely the analysis and ideas developed in [Chow & Sanders, 1986; Dumortier & Li, 2001; Gavrilov, 1993].

2. The planar Hamiltonian differential system

As we have mentioned above, this section is devoted to analyze the system (5), depending on c. Indeed, due to a rescaling, we can consider that $c = 1$, if $c > 0$, or $c = -1$, if $c < 0$. A straightforward analysis shows that, for the first case, the origin is a global center and, for the second case, the origin is a local center and there exist two saddle points located at $(-1, 0)$ and $(1, 0)$, with a heteroclinic orbit connecting them. See the qualitative phase portraits for each case in Fig. 1(i) and in Fig. 1(iv), respectively. The rest of the section describes the global behavior of the period function.

Let h_0 be defined in an analogous way as in Sec. 1 but for the Hamiltonian function (6) and let the periodic orbit be

$$\gamma_h := \{(x, y) \in \mathbb{R}^2; H(x, y) = h\}, \tag{7}$$

for any $h \in (0, h_0)$. Then, the period function can be computed by means of

$$T(h) := \int_{\gamma_h} \frac{dx}{y} = 2\int_{x^-(h)}^{x^+(h)} \frac{dx}{\sqrt{2h - x^2 - cx^4/2}} = 4\int_0^{x^+(h)} \frac{dx}{\sqrt{2h - x^2 - cx^4/2}}, \tag{8}$$

where $(x^-(h), 0)$ and $(x^+(h), 0)$ are the intersection points of γ_h with the x-axis. It is clear that, by the symmetry, we get $x^+(h) = -x^-(h)$, and the last equality in (8) holds. Note that $T(h)$ is an analytic function on $(0, h_0)$ and, since the center is nondegenerate, it can be expanded analytically near $h = 0$ for $h > 0$ (see [Villarini, 1992]). Therefore, $T(h)$ is defined in the interval $[0, h_0)$.

Remark 2.1. Due to the form of the period function (8), it clearly depends on c and we will denote it by $T_c(h)$. However, for simplicity in this section, we write it as $T(h)$.

The monotonicity of the period function $T(h)$ defined in (8) can be proved using the fact that it satisfies a second order Picard–Fuchs equation that will be given in Lemma 1, and $x(h) = T'(h)/T(h)$ satisfies a Riccati equation, as it will be shown in Corollary 2.1. Although system (5) has the double symmetry described in Remark 1.1, the proof of the following lemma will not use this fact. Moreover, as we will need the explicit expressions given in terms of the parameter c, we do not assume $c = 1$ in all technical results.

Lemma 1. *If $T(h)$ is the period function defined in* (8)*, then it satisfies the following homogeneous second order differential equation*

$$4h(4ch+1)T''(h)+4(8ch+1)T'(h)+3cT(h)=0, \tag{9}$$

for all $h\in[0,h_0)$.

Proof. In this case, we have the Hamiltonian function given in (6), and γ_h is as given in (7). First, we define the expression $I_j(h)=\int_{\gamma_h}x^j y dx$, for $j=0,1,2,\dots$, and obtain the Picard–Fuchs system of differential equations

$$\begin{pmatrix} I_0'' \\ I_2'' \end{pmatrix}=\frac{1}{\delta}\begin{pmatrix} 4h & -1 \\ -\frac{4h}{c} & -4h \end{pmatrix}\begin{pmatrix} I_0' \\ I_2' \end{pmatrix}, \tag{10}$$

where $\delta=-4h(4ch+1)/c$, with $\gamma_h=\{y^2+x^2+cx^4/2=2h\}$.

Since $T(h)=I_0'(h)$, then, by (10), the period map $T(h)$ satisfies the homogeneous second order differential equation (9). ■

A first straightforward consequence of the above result is the next corollary and, from it, we can describe the local behavior near the extrema of the function $T(h)$. Even though Lemma 2 can be used to obtain the series solution for the initial value problems of $x(h)$ and $T(h)$, we keep the present proof because it is necessary for proving Lemma 3.

Corollary 2.1. *Let $T(h)$ be a function satisfying* (9)*. Then, the function $x(h)=T'(h)/T(h)$ verifies the Riccati equation*

$$4h(4ch+1)x'(h)+4h(4ch+1)(x(h))^2+4(8ch+1)x(h)+3c=0, \tag{11}$$

for all $h\in[0,h_0)$.

Lemma 2. *Consider the period map $T(h)$ given in* (8)*, for $h\in[0,h_0)$. Then, $T(0)=2\pi$, $T'(0)=-3c\pi/2$, and*

$$T(h)=2\pi-\frac{3c\pi}{2}h+\frac{105c^2\pi}{32}h^2-\frac{1155c^3\pi}{128}h^3+o(h^4)$$

is the Taylor series of T around $h=0$.

Proof. By applying the change of variables $(x,y,t)\mapsto(x,-y,-t)$ and simultaneously transforming to polar coordinates $(x,y)=(r\cos\theta,r\sin\theta)$ in system (5), we obtain:

$$\begin{cases} \dot r = cr^3\sin\theta\cos^3\theta =: R(r,\theta), \\ \dot\theta = 1+cr^2\cos^4\theta =: \Theta(r,\theta). \end{cases} \tag{12}$$

Moreover, for h positive small enough, the radius $r_h(\theta)$ of γ_h, given by (7), is the unique solution of

$$\frac{dr}{d\theta}=\frac{R(r,\theta)}{\Theta(r,\theta)},$$

with initial condition $(r,\theta)=(x_r(h),0):=(r_0,0)$, where r_0 is the positive root of $x^2/2+cx^4/4=h$. As r_0 is also small enough, we can write the solution in power series. Then, $r_h(\theta)=r_0+\sum_{j=2}^{\infty}U_j(\theta)r_0^j$, for some trigonometric polynomials U_j. Substituting this last expression into the second equation of (12), there exist trigonometric polynomials V_j and S_j such that it can be written in the form $d\theta/dt=1+\sum_{j=1}^{\infty}V_j(\theta)r_0^j=\Theta(r_h(\theta),\theta)$ and, then, $dt=d\theta/\Theta(r_h(\theta),\theta)$. Consequently, we can compute the period of γ_h by

$$T(h):=T(r_h(\theta))=\int_0^{2\pi}\frac{1}{\Theta(r_h(\theta),\theta)}d\theta=2\pi+\sum_{j=1}^{\infty}S_j(\theta)r_0^j. \tag{13}$$

Hence, $T(0)=2\pi$ and the above series converges for $0<\theta\le 2\pi$ because $r_0\ge 0$ is sufficiently small.

If $c = 0$, then

$$T(h) = \int_0^{2\pi} d\theta = 2\pi,$$

for all h, and hence the center is isochronous.

Now, for $c \neq 0$, we can determine the values of the j-th derivatives $T^{(j)}(h)$ by using the Picard–Fuchs equation (9). In fact, considering $h = 0$ in (9), we obtain $T'(0) = -3c\pi/2$. Taking now the derivative of (9), we obtain

$$(16ch^2 + 4h)T^{(3)}(h) + (64ch + 8)T''(h) + 35cT'(h) = 0, \tag{14}$$

and by replacing $h = 0$ and $T'(0) = -3c\pi/2$, we can check that $T''(0) = 105c^2\pi/16$. Differentiating equation (14), we have

$$(16ch^2 + 4h)T^{(4)}(h) + (96ch + 12)T^{(3)}(h) + 99cT''(h) = 0. \tag{15}$$

Hence, by replacing $h = 0$ and $T''(0) = 105c^2\pi/16$ in equation (15), we obtain $T^{(3)}(0) = -3465c^3\pi/64$. We could continue this inductive procedure to determine all the higher order derivatives. ■

Lemma 3. *Assume that $c > 0$ in system (5) and its period function $T(h)$ is given by (8). Then, $T(h) \to 0$, as $h \to \infty$.*

Proof. We can assume, without loss of generality, that $c = 1$ and that (5), after the change $(x, y, t) \to (x, -y, -t)$, can be written in polar coordinates, leading to the system (12). From the expressions in (12), we have that, for any (r, θ), we have

$$\Theta(r, \theta) > 1 \Rightarrow \frac{1}{\Theta(r, \theta)} < 1. \tag{16}$$

Note also that the distance between γ_h and the origin tends to infinity as $h \to \infty$. The proof of Lemma 2 gives us a parametrization of the radius with respect to the angle, for any h, denoted by $r_h(\theta)$, and that we can compute the period of γ_h, for each h, by means of (13). On the other hand, note that, since $r(\theta, h) \to \infty$ as $h \to \infty$, for each θ, we have:

$$\lim_{h\to\infty} \frac{1}{\Theta(r(\theta, h), \theta)} = \begin{cases} 1, & \text{if } \theta = \pm\dfrac{\pi}{2}, \\ 0, & \text{otherwise.} \end{cases}$$

Therefore, by using (16), we can apply the Dominate Convergence Theorem and assert that $\lim_{h\to\infty} T(h) = 0$. ■

Aiming to make a complete study on the monotonicity of the period function $T(h)$, instead of the Riccati equation (11), we study the global phase portrait of the equivalent autonomous differential system on the plane. For this system, the phase curve $(h, x(h))$ has the following fundamental property: suppose that, for $h = \hat{h}$, the periodic solution $\gamma_{\hat{h}}$ vanishes. Then, $\lim_{h\to\hat{h}} T'(h)/T(h) = \hat{x} \neq \pm\infty$, the equilibrium point $(\hat{h}, \hat{x})$ is a saddle and the curve $(h, x(h))$ is a separatrix of $(\hat{h}, \hat{x})$. Consequently, after determining this phase curve and the isoclines, we can obtain the sign and behavior of $T'(h)$ in $[0, h_0)$. This is done using the ideas presented in [Gavrilov, 1993; Mañosas & Villadelprat, 2006].

Lemma 4. *Consider the period map $T(h)$ given in (8). Thus, if $c = 0$, then $T(h)$ is constant, if $c < 0$, then it is monotonically increasing, and if $c > 0$, then it is monotonically decreasing. Moreover, for $c \neq 0$, we have that $T'(h)$ is monotonically increasing, i.e. $T''(h) \geq 0$, for all $h \in [0, h_0)$.*

Proof. When $c = 0$, the center is linear and isochronous, and $T(h) = 2\pi$, for all h. When $c \neq 0$, we can define $x(h) = T'(h)/T(h)$, which verifies, by Corollary 2.1, the Riccati equation (11), for all $h \in [0, h_0)$. Instead of Eq. (11), we study an equivalent autonomous differential system on the plane given by

$$\begin{cases} \dot{h} = -4h(4ch + 1), \\ \dot{x} = 4h(4ch + 1)x^2 + 4(8ch + 1)x + 3c. \end{cases} \tag{17}$$

The roots of $-4h(4ch+1)=0$ are $h=0$ and $h=-1/(4c)$, and they correspond to invariant vertical straight lines on the (h,x)-plane. Moreover, for each c, $p_0=(0,-3c/4)$ and $p_1=(-1/(4c),3c/4)$ are equilibrium points of system (17). Its linear part at p_0 and at p_1 are

$$\begin{pmatrix} -4 & 0 \\ -\frac{87}{4}c^2 & 4 \end{pmatrix} \quad \text{and} \quad \begin{pmatrix} 4 & 0 \\ \frac{87}{4}c^2 & -4 \end{pmatrix},$$

respectively. Therefore, they are hyperbolic saddles, whose eigenvectors are $(1,87c^2/32)$ and $(0,1)$, respectively.

Remember that, for the analytical case, it is sufficient to consider $c=-1$, for $c<0$, and $c=1$, for $c>0$. We reproduce here all the computations for both cases, although the proof follows closely.

Now we describe the idea of the proof. First, we show that the graphic of $x(h)$ coincides with a separatrix of the saddle p_0. We denote such a separatrix by Γ and we represent it in Figs. 2 and 3 by the dotted line. Then, we identify the horizontal isoclines P_j and Q_j of (17) and we analyze the behavior of the vector field in the regions bordered by them. First, for $c=-1$, due to the fact that Γ reaches the saddle point with a slope less than the one of Q_1, and due to the behavior of the vector field in the regions determined by P_1 and Q_1, it follows that Γ is as on the right side in Fig. 2. Performing a similar analysis for $c=1$, now for P_2 and Q_2, we can only guarantee that Γ is below P_2. So, to prove that Γ is in the region between P_2 and Q_2, as represented on the right side of Fig. 3, we must find a special curve. Then, it is possible to determine the sign of the derivative of the period function in both cases.

Finally, for the proof of the second statement, it is enough to prove that $x'(h)>0$, for all $h\in[0,h_0)$, since from Lemma 2, $T''(0)=105c^2\pi/16>0$, and we have the following equivalences

$$x'(h)>0 \Leftrightarrow \frac{T''(h)T(h)-(T'(h))^2}{T(h)^2}>0 \Leftrightarrow T''(h)>\frac{(T'(h))^2}{T(h)}>0,$$

that is, $x'(h)>0$ if and only if $T''(h)>0$.

Case $c=-1$. The Hamiltonian differential system associated to the Hamiltonian function (6) has only the period annulus of the center at the origin, which is bounded. Moreover, $T(h)$ is defined for $h\in[0,h_0)$, where $h_0=-1/(4c)=1/4$. Then, $T(h)\to+\infty$ as $h\to 1/4$, and this implies that $T'(h)$ takes positive values as $h\to 1/4$.

Since $c=-1$, the invariant vertical straight lines of (17) are $h=0$ and $h=1/4$, which are drawn in gray on the Fig. 2, and the equilibrium points are saddles at $p_0=(0,3/4)$ and $p_1=(1/4,-3/4)$.

Consider the vertical strip $\mathcal{U}=\{(h,x);\ 0\le h\le 1/4,\ x\ge 0\}$ and notice that there exist a unique orbit Γ lying in the interior of $\mathcal{U}$ and having the saddle p_0 as an ω-limit point, that is, Γ is the stable separatrix of p_0, and it is drawn on the right side of Fig. 2, with dashed line.

We claim that the graphic of $x(h)$ coincides with the stable separatrix Γ. In fact, first by using the Taylor series obtained in Lemma 2, we have that the curve $x(h)=T'(h)/T(h)$, for $h\in(0,1/4)$, is an integral curve of system (17) that tends to $3/4$ as $h\to 0$, and this value is the x-component of p_0. Then, the statement follows from the uniqueness of solutions.

Now we can show that $T'(h)>0$ and $x'(h)>0$, for all $h\in[0,1/4)$.

For $h=0$, we have that $x'(0)=87/32$ (this is simply obtained by computing the slope of the eigenvectors at the saddle point p_0). Now, consider the second equation in (17) equals to 0, then we obtain the points where the vector field is horizontal. This equation defines two curves given by

$$P_1(h)=\frac{-8h+1+\sqrt{52h^2-13h+1}}{2h(4h-1)} \quad \text{and} \quad Q_1(h)=\frac{-8h+1-\sqrt{52h^2-13h+1}}{2h(4h-1)},$$

whose connected components are graphics of functions in h. The curve P_1 is drawn in blue and Q_1 is drawn in purple in Fig. 2. The vector field is transversal to P_1 and Q_1.

We now study the position of P_1 and Q_1 with respect to Γ. The curves P_1 and Q_1 divide the vertical strip $\mathcal{U}$ into two regions where the vector field points upward in the top and points downward in the bottom region (see Fig. 2).

At p_0, the limit of the slopes of the tangent lines to Q_1 as h tends to 0 is equal to $87/16$, which is bigger than the slope $x'(0)=87/32$ of Γ at the same point. Then, in a neighborhood of p_0, the separatrix

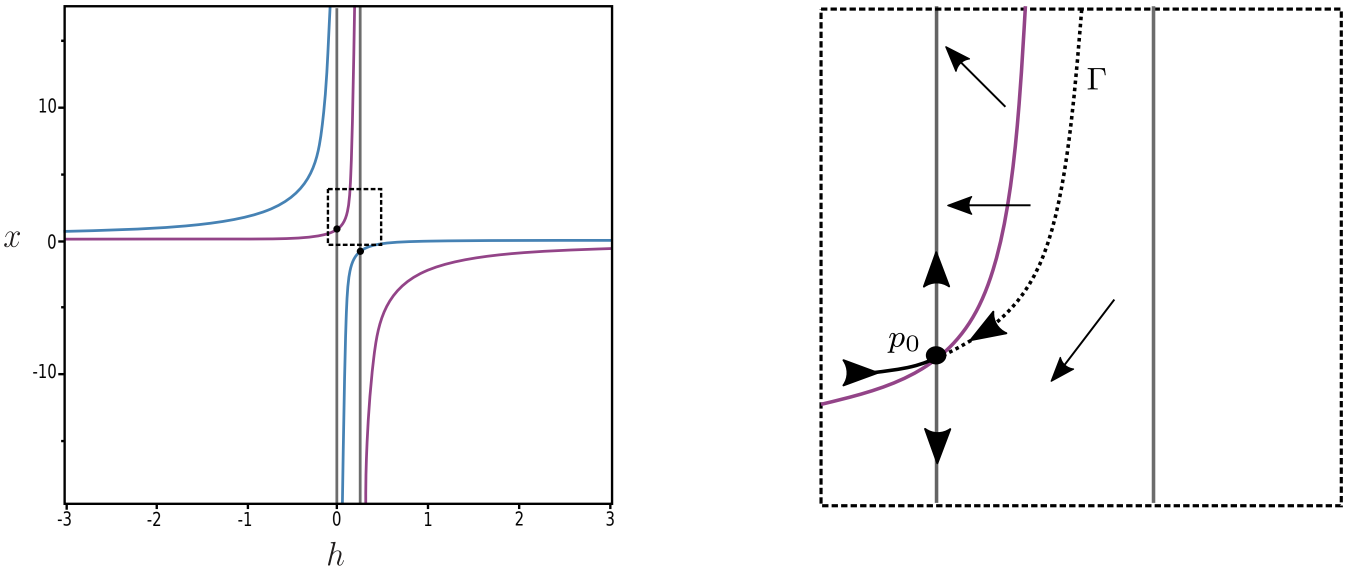

Fig. 2. Invariant vertical straight lines (in gray), curves P_1 (in blue) and Q_1 (in purple) and relative position of Γ

Γ is bellow Q_1. Since the vector field is transversal to Q_1 and it is directed to the left, the orbit Γ is not allowed to intersect Q_1 for $t \to -\infty$, and the orbit Γ is always bellow Q_1. Moreover, Γ is above the h-axis since the vector field points downward on $(0, 1/4) \times \{0\}$, because the second component of the vector field is constant and it is equal to -3. Therefore, the graphic of $x(h)$, which is the orbit Γ, is entirely located in $\mathcal{U}$. This implies that $x(h) = T'(h)/T(h) > 0$, then $T'(h) > 0$, for all $h \in [0, 1/4)$. We also have that $x'(h) = (dx/dt)/(dh/dt) > 0$, since $dx/dt < 0$ in the region bellow Q_1 in the vertical strip $\mathcal{U}$ and $dh/dt < 0$, for all $h \in [0, 1/4)$.

Case $c = 1$. We already know that the planar Hamiltonian differential system (5) associated to the Hamiltonian function (6) has only the period annulus of the center at the origin, which is global. Moreover, the corresponding period function is defined for $h \in [0, \infty)$. As the analysis for this case is very similar to the previous one, we only point out the main differences. Now the invariant vertical straight lines of (17) are $h = 0$ and $h = -1/4$, which are drawn in gray on the Fig. 2, the saddle equilibrium points are $p_0 = (0, -3/4)$ and $p_1 = (-1/4, 3/4)$, and $\mathcal{U} = \{(h, x); h \geq 0\}$ is a half-plane. Again Γ is the stable separatrix of p_0 and it is drawn on the right side of Fig. 3 with dashed line and it is the graphic of $x(h)$. Moreover, the curve $x(h) = T'(h)/T(h)$, for $h \in (0, +\infty)$, is an integral curve of system (17) that tends to $-3/4$ as $h \to 0$, and this value is the x-component of p_0.

Analogously, we show that $T'(h) < 0$ and $x'(h) > 0$, for all $h \in [0, \infty)$. We have that $x'(0) = 87/32$ and the horizontal isocline is defined by the graphics of the next two functions:

$$P_2(h) = \frac{-8h - 1 + \sqrt{52h^2 + 13h + 1}}{2h(1 + 4h)} \quad \text{and} \quad Q_2(h) = \frac{-8h - 1 - \sqrt{52h^2 + 13h + 1}}{2h(1 + 4h)}.$$

They are drawn in blue and in purple, respectively, in Fig. 3. The vector field is transversal to P_2 and Q_2 and it is directed to the left.

In this case, the curves P_2 and Q_2 divide $\mathcal{U}$ into three regions where the vector field points upwards on the top and on the bottom regions, and it points downward on the middle region (see Fig. 3). The limit of the slopes of the tangent lines to P_2 as h tends to 0 is equal to $87/16$, which is bigger than the slope $x'(0) = 87/32$ of Γ. Then, near p_0, the separatrix Γ is under P_2. Using the transversality and the direction of the vector field to P_2, the orbit Γ cannot intersect P_2 again for $t \to -\infty$. The orbit Γ is then entirely located in $\mathcal{U}$, bellow P_2.

Proving that Γ is above the curve Q_2 requires a more accurate analysis. Some calculations show that

$$\lim_{h \to 0^+} P_2(h) = -3/4, \lim_{h \to +\infty} P_2(h) = 0, \lim_{h \to 0^+} Q_2(h) = -\infty, \text{ and } \lim_{h \to +\infty} Q_2(h) = 0.$$

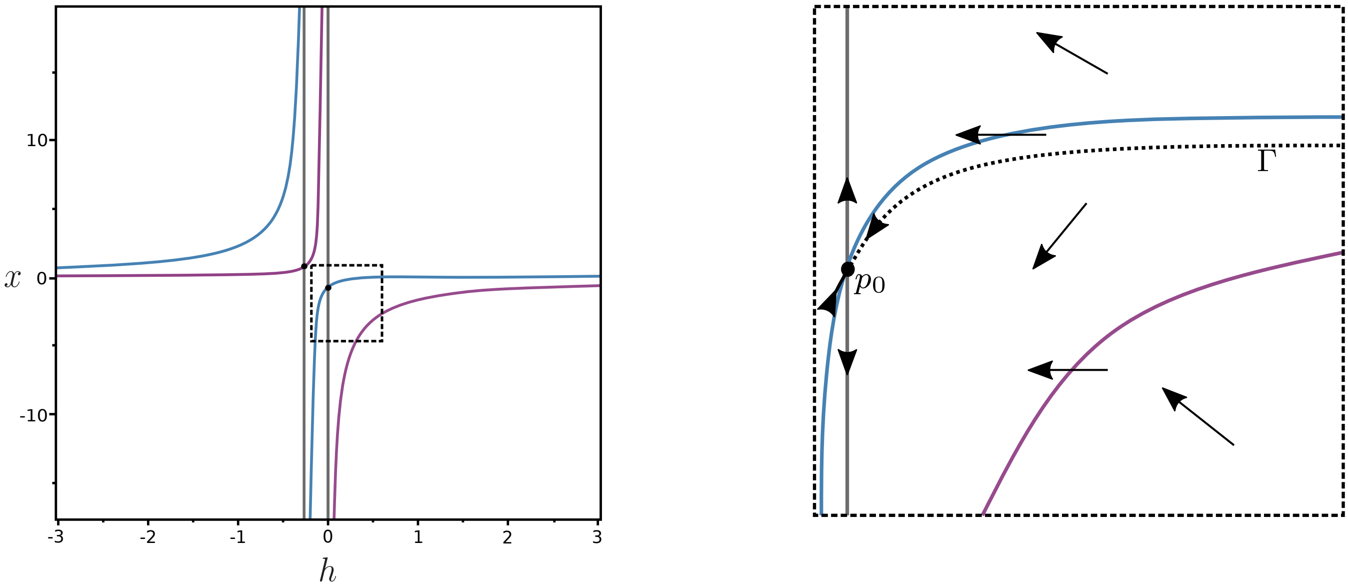

Fig. 3. Invariant vertical straight lines (in gray), curves P_2 (in blue) and Q_2 (in purple) and relative position of Γ

Now, notice that any convex combination

$$R_s(h) = sP_2(h) + (1-s)Q_2(h),$$

with $s \in [0,1]$, is a curve that has the following properties: $R_s(h)$ is monotonically increasing, $Q_2(h) \leq R_s(h) \leq P_2(h)$, for all $h \in [0,\infty)$,

$$\lim_{h\to\infty} R_s(h) = 0, \text{ and } \lim_{h\to 0^+} R_s(h) = -\infty.$$

Consider $s^* = 7/8 \in [0,1]$, then the curve Γ is in the region between the curves R_{s^*} and P_2, and then we will conclude that Γ is above the curve Q_2. In fact, $R_{s^*}(h) = 7P_2(h)/8 + Q_2(h)/8$, whose graphic is the zero level curve of the function

$$F(h,x) = 2xh(4h+1) + 8h + 1 - 3\sqrt{52h^2+13h+1}/4,$$

i.e. $(h, R_{s^*}(h)) := \{(h,x) \colon F(h,x) = 0\}$.

In the region near the saddle point p_0, the curve R_{s^*} is below Γ, since $x(0) = -3/4$, $\lim_{h\to 0^+} R_{s^*}(h) = -\infty$, and R_{s^*} is monotonically increasing. Moreover, by solving the equation $R_{s^*}(h) = -3/4$, it follows that the curve R_{s^*} intersects the line $x = -3/4$ at the point $(1/3, -3/4)$.

Note that the gradient of F is given by

$$\nabla F = \left(2x(4h+1) + 8xh + 8 - \frac{3(104h+13)}{8\sqrt{52h^2+13h+1}}, 2h(4h+1)\right),$$

and it is always orthogonal to R_{s^*}, and it is directed upward. Since

$$\left\langle \nabla F, (\dot{h}, \dot{x}) \right\rangle \Big|_{F=0} = \frac{5}{8}(132h^2+33h+5) - \frac{3(8h+1)(52h^2+13h+2)}{2\sqrt{52h^2+13h+1}} \tag{18}$$

is always negative for $h \in (1/3,\infty)$, because evaluating (18) at $h = 1$ we get $425/4 - 603\sqrt{66}/44 < 0$, and since the polynomial that is obtained by eliminating the root by squaring has no roots in the interval $(1/3,\infty)$, then the angle formed by ∇F and $(\dot{h}, \dot{x})$ is greater than $\pi/2$, for all $h \in (1/3,\infty)$. So, the behavior of the vector field (17) along the curve R_{s^*} is as presented in Fig. 4.

Then, the region in gray on the left side of Fig. 4 is a trapping region for system (17), i.e. solutions that start inside this region (including on its boundary) stay inside of it for all negative times. Thus, the curve Γ remains above the curve R_{s^*}, for all $h \in [0,\infty)$, implying that the curve Γ is above Q_2.

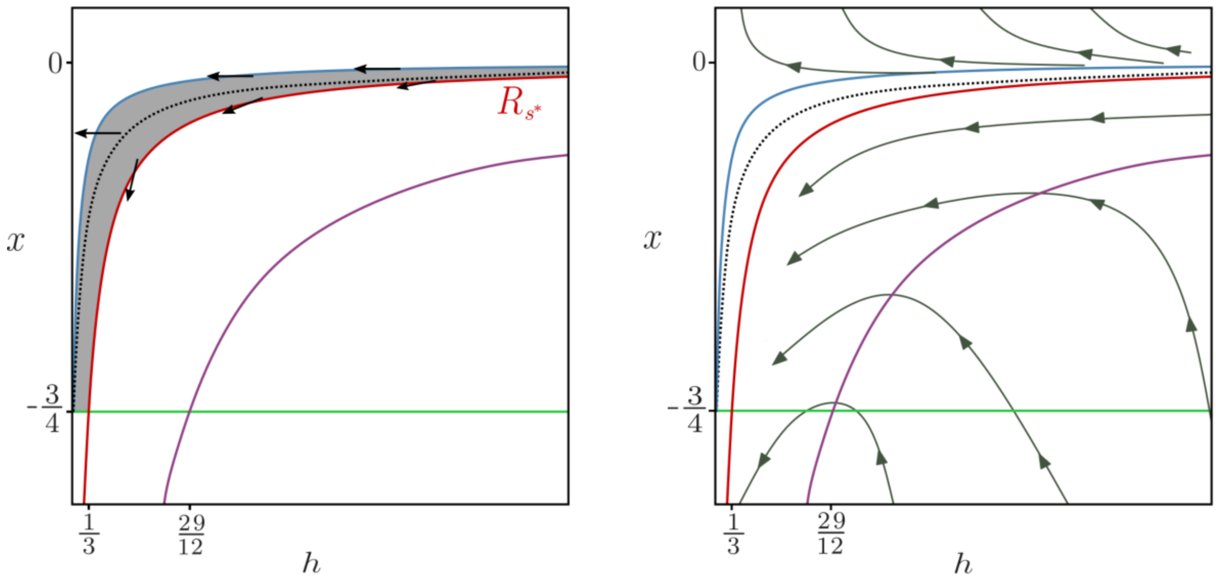

Fig. 4. Region negatively invariant in gray and curve R_{s^*} in red

Therefore, the graphic of x is located below the h-axis, between P_2 and Q_2. Since it is bellow P_2, the second component $T'(h)/T(h) < 0$, for all $h \in [0, \infty)$, so $T'(h) < 0$, for all $h \in [0, \infty)$. Moreover, this implies that $x'(h) = (dx/dt)/(dh/dt) > 0$, since $dx/dt < 0$ in the region between P_2 and Q_2 and $dh/dt < 0$, for all $h \in [0, \infty)$. $\blacksquare$

3. Proof of Proposition 1

Family (2) has a center at the origin because its solutions are invariant with respect to the change of variables $(x, y, t) \to (-x, y, -t)$. Before we consider the case-by-case study, we will describe the critical levels of the Hamiltonian function (3).

In order to determine h_0, we study the graphic of $V^-(x) = x^2/2 + ax^4/4$, for $x \le 0$, and $V^+(x) = x^2/2 + bx^4/4$, for $x \ge 0$, defined in (4), as it was done in [Mañosas & Villadelprat, 2006].

The critical levels of (3), for $x \le 0$ (resp. $x \ge 0$), are the positive zeros of the discriminant of $V^-(x) - h$ (resp. $V^+(x) - h$) with respect to x, that is, the common solutions of $(V^-)'(x) = 0$ and $V^-(x) = h$ (resp. $(V^+)'(x) = 0$ and $V^+(x) = h$). As we have that such discriminants are equal to $-ah(1+4bh)^2/4$ for V^+, and $-bh(1+4ah)^2/4$ for V^-, the union of the zeros of the two discriminants is $\{0\}$, if a and b are zero, $\{0, h^-, h^+\}$, where $h^- = -1/(4a)$ and $h^+ = -1/(4b)$, if a and b are nonzero, $\{0, h^+\}$, if $a = 0$, or $\{0, h^-\}$, if $b = 0$.

To completely analyze the systems, we study five different cases in terms of the signs of the parameters a and b. The first three cases are those ones when the two parameters have the same signs, and the last two cases correspond to the cases when the two parameters have different signs.

Case 1. For $a \ge 0$ and $b \ge 0$: Note first that both systems of the form (5) associated to the Hamiltonian function given by (6) with $c = a$, for the left half-plane, and with $c = b$, for the right half-plane, have a global center at the origin. Then, the piecewise system also has a global center at the origin and the graphic of V and the phase portrait are represented by (i) in Fig. 1.

Case 2. For $a < 0$, $b < 0$ and $|a| \ne |b|$: The Hamiltonian function given by (6) with $c = a$ (resp. $c = b$) is a first integral of the system (5) in the left (resp. right) half-plane, then there exist one saddle for $x \le 0$ (resp. $x \ge 0$) in the level h^- (resp. h^+), and a center at the origin. Since $|a| \ne |b|$, $h^- \ne h^+$ are two positive values and then $h_0 = \min\{h^-, h^+\}$. Therefore, $\partial\mathcal{P}$, which is contained in the level curve with h_0, has one saddle with a finite homoclinic connection. The graphic of V and the phase portrait are represented by (iii) in Fig. 1.

Case 3. For $a < 0$, $b < 0$ and $|a| = |b|$: The Hamiltonian function given by (6) with $c = a$ (resp. $c = b$) is a first integral of the system (5) in the left (resp. right) half-plane, then there exists one saddle, for $x \leq 0$ (resp. $x \geq 0$) at the level h^- (resp. h^+), and a center at the origin. Since $|a| = |b|$, then $h_0 = h^- = h^+$. Therefore, system (2) has two saddles with a finite heteroclinic connection between them at the level h_0. The graphic of V and the phase portrait are represented by (iv) in Fig. 1.

Case 4. For $a < 0$ and $b \geq 0$: The Hamiltonian function given by (6) with $c = a$ (resp. $c = b$) is a first integral of the system (5) in the left (resp. right) half-plane. Then, there exist a center at the origin and a saddle at the level h^-, for $x \leq 0$, and only a center at the origin for $x \geq 0$. Therefore, there exists a positive value $h_0 = \max\{h^-, h^+\}$. The graphic of V and the phase portrait are represented by (ii) in Fig. 1.

Case 5. For $a \geq 0$ and $b < 0$: This case can be obtained by the previous one by using the change of variables $(x, y, t) \mapsto (-x, y, -t)$.

In summary, Cases $1, 2, 3$ correspond to items (i), (iii), (iv) in Proposition 1 and Cases 4 and 5 to item (ii).

4. The period function for the piecewise system

By using the expression of the period of the continuous case in (8) and the fact that system (2) is symmetric with respect to the x and y-axis, the next result follows.

Lemma 5. *The period function of system* (2)*, defined in* $[0, h_0)$*, is*

$$T(h) = \frac{1}{2}\big(T_a(h) + T_b(h)\big), \tag{19}$$

where $T_c(h)$ *is defined in* (8) *(see Remark 2.1).*

Since $T'(h) = \big(T'_a(h) + T'_b(h)\big)/2$ and $T''(h) = \big(T''_a(h) + T''_b(h)\big)/2$, from Lemmas 2 and 4, we obtain the following result.

Lemma 6. *Consider the period function* $T(h)$ *given in* (19)*. Then,* $T(0) = 2\pi$, $T'(0) = -3\pi(a+b)/4$*, and* $T''(h) > 0$*, for all* $h \in [0, h_0)$.

We want to highlight that next corollary shows that the sum of two functions satisfying each a different Picard–Fuchs equation of order 2 is the solution of another Picard–Fuchs equation but of order 4. The proof follows straightforwardly. Obviously, this property can be extended to higher orders.

Corollary 4.1. *If* $T(h)$ *is the period function of* (2)*, then* $P_4(h)T^{(4)}(h) + P_3(h)T^{(3)}(h) + P_2(h)T''(h) + P_1(h)T'(h) + P_0T(h) = 0$*, for all* $h \in [0, h_0)$*, where*

$$\begin{aligned}
P_4(h) &= 16h^2\big[256a^3bh^4 + 64(a+3b)a^2h^3 + 48(a+b)ah^2 + 4(3a+b)h + 1\big],\\
P_3(h) &= 8h\big[3584a^3bh^4 + 32(19a+75b)a^2h^3 + 48(8a+11b)ah^2 + 2(39a+19b)h + 5\big],\\
P_2(h) &= 41472a^3bh^4 + 64(61a+385b)a^2h^3 + 16(127a+284b)ah^2 + 4(71a+61b)h + 5,\\
P_1(h) &= 8448a^3bh^3 + 176(a+25b)a^2h^2 + 88(a+7b)ah + 11(a+b),\\
P_0(h) &= 528a^3bh^2 + 264a^2bh + 33ab.
\end{aligned}$$

We finish this paper proving Theorem 1. We observe that we will not use the above result because of the difficulties dealing with the solutions of a differential equation of order four.

First, if $a = 0$ and $b = 0$, then the center is linear and isochronous, T is constant and it is equal to 2π. As a matter of fact, we can further reduce the number of parameters to one, when $b \neq 0$ using the following rescaling $x \to \lambda x$, $y \to \lambda y$ in system (2) and we assume that in the right hand side we have $b = 1$ or $b = -1$.

For the case $a \geq 0$ and $b > 0$, i.e. $b = 1$, using Proposition 1(i), the origin is a global center and $h_0 = \infty$, then the period function is defined in $[0, \infty)$ and, by Lemma 6, $T'(0) = -3\pi(a+1)/4 < 0$. Moreover, by Lemma 4, $T'_a(h) < 0$ and $T'_b(h) < 0$, for all $h \in (0, \infty)$. Thus, $T'(h) = T'_a(h) + T'_b(h) < 0$, $T''(h) > 0$

from Lemma 6, and $\lim_{h\to\infty} T(h) = 0$ from Lemma 3, hence T is monotonically decreasing, convex and its graphic is as represented in the blue region in Fig. 5.

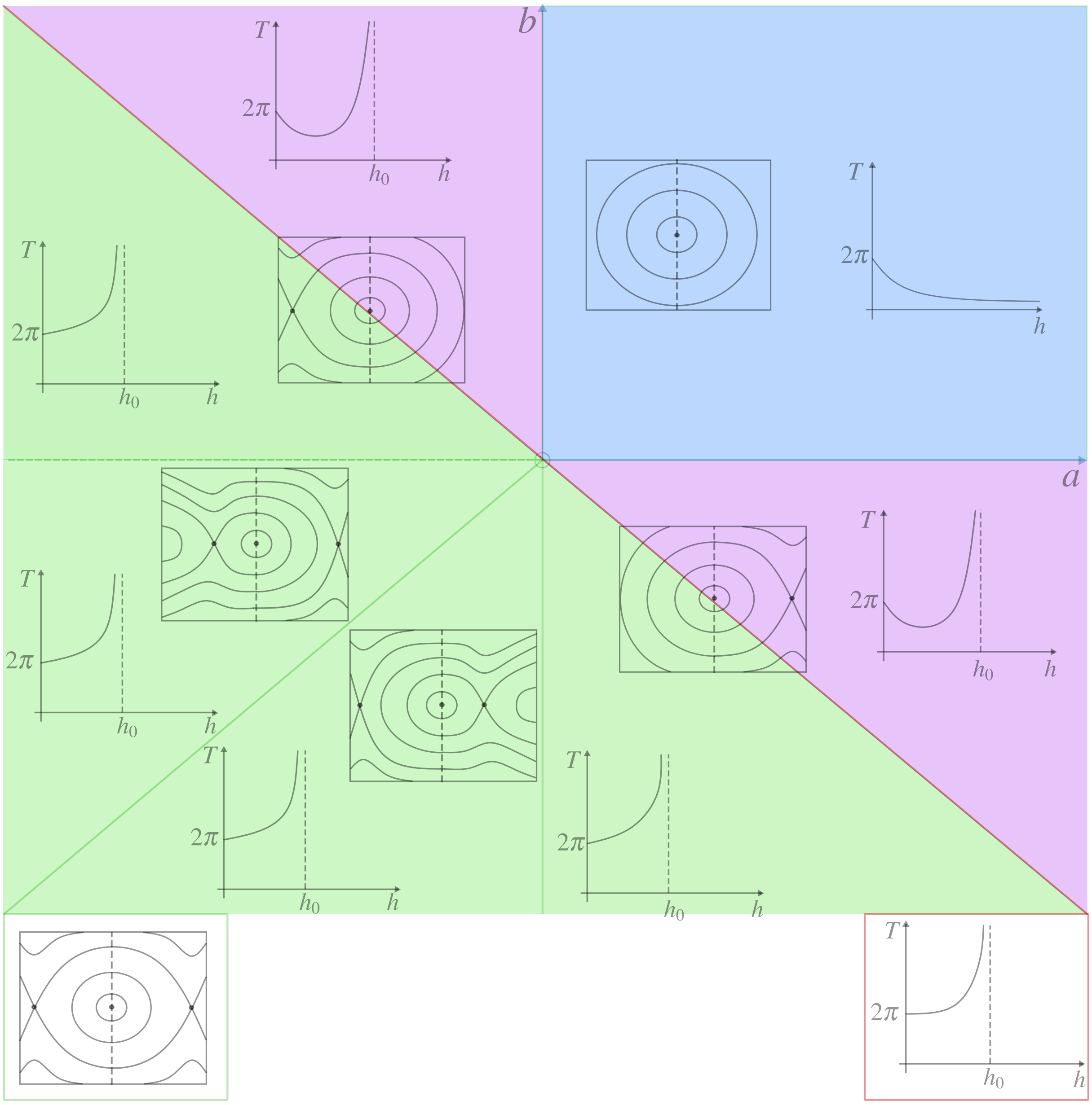

Fig. 5. Bifurcation diagram of the period function of the center at the origin of system (2)

In the case $a < 0$ and $b < 0$, i.e. $b = -1$, the period function is defined in $[0, h_0)$, with $h_0 = \min\{-1/(4a), 1/4\}$ by items (iii) and (iv) in Proposition 1. Lemma 6 implies $T'(0) = -3\pi(a-1)/4 > 0$ and Lemma 4 that $T_a'(h) > 0$ and $T_b'(h) > 0$ for all $h \in [0, h_0)$. Thus, $T'(h) = T_a'(h) + T_b'(h) > 0$, and hence T is monotonically increasing. Moreover, it is convex, $T''(h) > 0$, from Lemma 6, with a horizontal asymptotic straight line in $h = h_0$. Therefore, the graphic of T is as represented in the green region in Fig. 5.

For the last cases, $ab < 0$, we can assume that $a < 0$ and $b > 0$ by symmetry and, as above, we take $b = 1$. By Proposition 1(ii) and Lemma 6 we have that the period function is defined in $[0, h_0)$, where $h_0 = \max\{-1/(4a), -1/4\} = -1/(4a)$,

$$T'(0) = \frac{-3\pi(a+1)}{4}, \tag{20}$$

and $T''(h) > 0$, for all $h \in [0, h_0)$. First suppose that $|a| > 1$, then we have $T'(0) > 0$, by equation (20), since $T'(h) > 0$ and $T''(h) > 0$, for all $h \in [0, -1/(4a))$ the period function is convex and monotonically increasing, whose graphic is represented in the green region in Fig. 5. When $a = -1$, we have $T'(0) = 0$ by equation (20), $T'(h) > 0$ and $T''(h) \geq 0$, for all $h \in (0, 1/4)$. Consequently the graphic of T is as represented in the red square in Fig. 5. Now take $|a| < 1$, thus we have $T'(0) < 0$ by (20), and since $T''(h) > 0$, for all $h \in [0, -1/(4a))$, the period function has one simple critical period, which is a minimum point. Furthermore, the derivative T' cannot have a horizontal asymptotic straight line at 0. In fact, as $a < 0$, it is known that $\lim_{h\to h_0} T_a(h) = \infty$, where $h_0 = -1/(4a)$. Then $\lim_{h\to h_0} T(h) = \lim_{h\to h_0}(T_a(h) + T_b(h))/2 = \infty$ and, therefore, $T'(h) > 0$, when $h \to h_0$. It follows that the graphic of T is as represented in the purple region in Fig. 5.

Acknowledgments

This work has been realized thanks to the Brazilian CAPES (Coordenação de Aperfeiçoamento de Pessoal de Nível Superior - Finance Code 001) and FAPESP (grant 2019/21181-0) agencies; the Catalan AGAUR agency (grant 2021SGR00113); the Spanish Ministerio de Ciéncia, Innovación y Universidades, Agencia Estatal de Investigación (grants PID2022-136613NB-I00 and CEX2020-001084-M); and the European Union's Horizon 2020 research and innovation programme (grant Dynamics-H2020-MSCA-RISE-2017-777911).

References

Chen, X. & Zhang, W. [2012] "Isochronicity of centers in a switching Bautin system," *J. Differential Equations* **252**, 2877–2899.

Chicone, C. [1987] "The monotonicity of the period function for planar Hamiltonian vector," *J. Differential Equations* **69**, 310–321.

Chow, S.-N. & Sanders, J. A. [1986] "On the number of critical points of the period," *J. Differential Equations* **64**, 51–66.

Cima, A., Mañosas, F. & Villadelprat, J. [1999] "Isochronicity for several classes of Hamiltonian systems," *J. Differential Equations* **157**, 373–413.

Coll, B., Prohens, R. & Gasull, A. [1999] "The center problem for discontinuous Liénard differential equation," *Int. J. Bifurcation Chaos Appl. Sci. Eng.* **9**, 1751–1761.

Dumortier, F. & Li, C. [2001] "Perturbations from an elliptic Hamiltonian of degree four. I: Saddle loop and two saddle cycles," *J. Differential Equations* **176**, 114–157.

Filippov, A. F. [1988] *Differential equations with discontinuous righthand sides* (Kluwer Academic Publishers Group, Dordrecht).

Gasull, A., Guillamon, A., Mañosa, V. & Mañosas, F. [1997] "The period function for Hamiltonian systems with homogeneous nonlinearities," *J. Differential Equations* **139**, 237–260.

Gasull, A. & Torregrosa, J. [2003] "Center-focus problem for discontinuous planar differential equations," *Int. J. Bifurcation Chaos Appl. Sci. Eng.* **13**, 1755–1765.

Gavrilov, L. [1993] "Remark on the number of critical points of the period," *J. Differential Equations* **101**, 58–65.

Li, F., Yu, P., Tian, Y. & Liu, Y. [2015] "Center and isochronous center conditions for switching systems associated with elementary singular points," *Commun. Nonlinear Sci. Numer. Simul.* **28**, 81–97.

Mañosas, F. & Torres, P. J. [2005] "Isochronicity of a class of piecewise continuous oscillators," *Proc. Amer. Math. Soc.* **133**, 3027–3035.

Mañosas, F. & Villadelprat, J. [2006] "A note on the critical periods of potential systems," *Int. J. Bifurcation Chaos Appl. Sci. Eng.* **16**, 765–774.

Villarini, M. [1992] "Regularity properties of the period function near a center of a planar vector field," *Nonlinear Anal.* **19**, 787–803.

Wang, S. & Yang, J. [2020] "Period functions and critical periods of piecewise linear system," *Electron. J. Differ. Equ.* **79**, 12 p.